Available online at www.sciencedirect.com

ScienceDirect

Ceramics International 40 (2014) 4655–4662

CERAMICS INTERNATIONAL

www.elsevier.com/locate/ceramint

Tribological properties of titania nanofilms coated on glass surface by the sol–gel method

Guojun Ji[a,*], Zhiming Shi[b], Wei Zhang[a], Ge Zhao[b]

[a]College of Chemical Engineering, Inner Mongolia University of Technology, Hohhot 010051, China
[b]School of Materials Science and Engineering, Inner Mongolia University of Technology, Hohhot 010051, China

Received 23 June 2013; received in revised form 1 September 2013; accepted 2 September 2013
Available online 8 September 2013

Abstract

Ce^{3+}-doped and undoped TiO_2 nanofilms with one, three, and five layers were prepared on glass surface by the sol–gel method. The thicknesses were about 40, 120 and 200 nm. Atomic force microscopy analysis showed that many defects existed on uncoated glass substrate surface such as microcracks and microvoids, resulting in high surface roughness. After coating with the TiO_2 nanofilms, the microdefects of the glass surface were filled and covered by film materials. With increased film layers and Ce^{3+} doping, the structure of the TiO_2 nanofilms surface became more uniform and compact, and the surface roughness gradually decreased. Nanoindentation and friction wear tests on the samples surface revealed that the surface hardness and friction coefficient of uncoated glass substrate were about 6.8 GPa and 0.37. After coating, the surface hardness of the samples increased and the friction coefficient remarkably decreased. Furthermore, with increased film thickness and Ce^{3+} doping, the friction coefficient of the sample gradually decreased and its wear-resisting property obviously increased. TiO_2 nanofilms coated on the glass substrate surface can be used as protective layers of glass, exerting excellent anti-wear and friction reducing effects.

Keywords: A. Films; C. Friction; D. Glass; D. TiO_2

1. Introduction

Titania nanofilms possess many unique properties such as high refractive index, dielectric constant, and photocatalytic activity [1–3]. After doping with rare-earth elements (such as Yb, Ce, Eu and Sm), the physical and chemical properties of these films can further be improved [4–6]. In recent years, the applications of titania nanofilms in the fields of self-cleaning, sensors, photocatalysis, and solar cells have been extensively studied [7–15]. However, most of these works have mainly focused on the control of phase composition, crystal texture and grain size of titanium oxide with the aim of improving the properties of titanium oxide film, such as photocatalysis, hydrophilicity, and photovoltaic conversion. Studies on the mechanical properties (e.g., surface hardness and frictional wear) of titania films, especially those mixed with rare-earth elements (e.g., Ce) are limited. These properties crucially influence the applications of such nanofilms.

Liu et al. [16] reported that the hardness of 5.0 mol% Au–TiO_2 films on glass increased from 3.61 to 6.48 GPa as the sintering temperature increased from 300 to 500 °C. After sintering at 500 °C, the 5.0 mol% Au–TiO_2 films coated on Si (1 0 0) substrate displayed better tribological properties than pure TiO_2 films. The friction coefficient was as low as 0.10 and the wear life exceeded 2000 sliding cycles. While the pure TiO_2 film showed a relatively higher friction coefficient (0.17) and a relatively shorter wear life (only 700 sliding cycles). Piwoński [17] investigated the influence of the porosity level on the tribological properties of titanium dioxide thin films. The results showed that with the increase of the average pore diameter of films from 100 to 300 nm, the friction coefficient and roughness of films increased from 0.02 to 0.37 and from 1.38 to 12.83 nm, respectively. Jia et al. [18] studied the tribological properties of TiO_2 sol–gel thin films on glass substrates sliding against Si_3N_4 ball. They found that the wear life of pure TiO_2 films was 2100 sliding cycles, and the wear life of the films doped with 17.9 mol% SiO_2 increased to 4300 sliding cycles. However, excessive SiO_2 doping deteriorated the wear resistance of the films. The wear life of TiO_2 films

*Corresponding author. Tel./fax: +86 471 6575722.
E-mail address: jgj@imut.edu.cn (G. Ji).

0272-8842/$ - see front matter © 2013 Elsevier Ltd and Techna Group S.r.l. All rights reserved.
http://dx.doi.org/10.1016/j.ceramint.2013.09.006

doped with 25 mol% SiO_2 was only about 700 sliding cycles. Rayón et al. [19] presented a nanoindentation study on the mechanical properties of TiO_2 coatings sprayed onto glass substrates. They found that the coatings consisted of anatase nanocrystals and rutile+anatase micro particles displayed a hardness of 8.5 GPa and 16.5 GPa, respectively. The higher friction coefficient obtained on the anatase surface ($\mu=0.7$) compared with that obtained on the anatase+rutile surface ($\mu=0.3$). The results showed that higher concentrations of anatase, which was softer than rutile, reduced the scratch damage and increased the friction coefficient of the TiO_2 coatings. Wang et al. [20] found that TiO_2 films were effective in improving the wear resistance and reducing the friction coefficient of glass substrates. But UV irradiation would worsen tribological properties of TiO_2 films. After the film was irradiated by UV, the friction coefficient between the film and GCr15 steel ball increased about 10%–50% and its wear life shortened about 20%–90%. In addition, Wan et al. [21] reported that sol–gel TiO_2 thin films modified with fluoroalkylsilane showed good friction-reducing and wear-protection behavior. It was found that the bare glass substrate was easily worn off during sliding. Under normal load of 0.5 N, friction coefficient was 0.8. Friction coefficient of the TiO_2 thin film was about 0.25 and could remain for a relatively long period (150 s) at initial stage before it reaches to 0.8. The best protection performance was observed at TiO_2–FAS film on glass substrate. Under the same testing condition, the modified film further decreased friction coefficient to 0.20 and the small friction coefficient remained almost unchanged even at an extended sliding cycle of 500 s before the film was worn out.

Therefore, it can be seen that investigations on the mechanical properties of TiO_2 films have gradually attracted researcher's attention, but few of them have focused on the effects of Ce-doping and thickness of the films on the surface mechanical properties of TiO_2 films. In fact, cerium, as the most abundant rare earth metal sensitizer in nature, has the same 4f electron configuration with titanium, which adds to reduce the crystallization temperature of TiO_2 and to inhibit the growth of TiO_2 crystals as well as improve the surface microstructure and mechanical properties of TiO_2 films. In this paper, a nanoindentation tester and a friction-wear tester were used to measure the hardness and tribological properties of glass surface uncoated and coated with sol–gel titania nanofilms. The effects of film thickness as well as Ce^{3+} doping on the surface morphology and tribological performance of the titania nanofilms were studied.

2. Experimental procedures

2.1. Preparation of samples

Tetrabutyl titanate, absolute alcohol, and cerium nitrate were used as precursor materials to prepare two kinds of sols with and without Ce^{3+} addition. First, tetrabutyl titanate was hydrolyzed in absolute alcohol, and then hydrochloric acid was added as a catalyst. The mixture was vigorously stirred with a magnetic stirrer for 30 min at room temperature. The volume composition was 1:6:0.1 $Ti(OC_4H_9)_4$:C_2H_5OH:HCl. The hydrolyzed tetrabutyl titanate sol was equally divided into two portions and injected into two beakers. Cerium nitrate ethanol solution was added to one of the beakers to prepare the mixed sol with 1:10 (molar ratio) $Ce(NO_3)_3.6H_2O$: Ti $(OC_4H_9)_4$. The finished sols were further stirred for 30 min, and then aged at room temperature for 24 h. The cleaned glass substrates were dipped into the sols and then withdrawn at a speed of 10 mm/min to form gel films on them. The film-deposited substrates were dried at 100 °C for 30 min, and subsequently sintered at 500 °C for 2 h in air to achieve crystallization of titania films. Finally, the multi-layer films were obtained by properly repeating the above procedures.

2.2. Characterization of films

The film thickness was measured with a scanning electron microscopy (SEM) system (S-3400, Hitachi). The crystal structure of the films were examined by an X-ray diffraction (XRD) instrument (D/Max-2500, Rigaku) with CuKα radiation at 40 kV, 120 mA, and 3°/min scanning speed. The surface morphology of the samples was observed by an atomic force microscopy (AFM) system (PicoScan AFM/STM, Veeco) at a scanning rate of 1.0 Hz.

2.3. Measurement of mechanical properties

The surface microhardness of the samples was measured on a nano-indenter (G200, Agilent Technologies) equipped with a three-sided pyramid (Berkovich diamond) tip. For each sample, indentation was conducted at 5 different locations.

The tribological properties of the samples were evaluated on a SFT type pin-on-disc friction and wear tester under dry sliding conditions. The counterpart AISI 52100 steel ball with a diameter of 5 mm was loaded against the rotating disk at a speed of 300 r/min. The normal load was 3 N. All tests were performed for 10 min, and the temperature and relative humidity were 25 °C and 30%, respectively. Prior to the tests, all samples were cleaned in an ultrasonic bath with ethanol and dried in hot air. The friction coefficient was automatically recorded. Throughout the entire friction process, the friction coefficient remained stable for a certain period and then sharply increased. The film was deemed to fail at this point, and the corresponding sliding cycle numbers or time was recorded as the wear life. Three replicate tests were carried out for each sample, and the average friction coefficient and wear life were obtained. Afterwards, the worn surfaces of the samples were observed with SEM.

3. Results and discussion

3.1. Thickness of films

Fig. 1 shows the cross-section images of the glass samples. It can be seen that the thicknesses of one-, three-, and five-layer TiO_2 nanofilms were approximately 40, 120, and 200 nm, respectively.

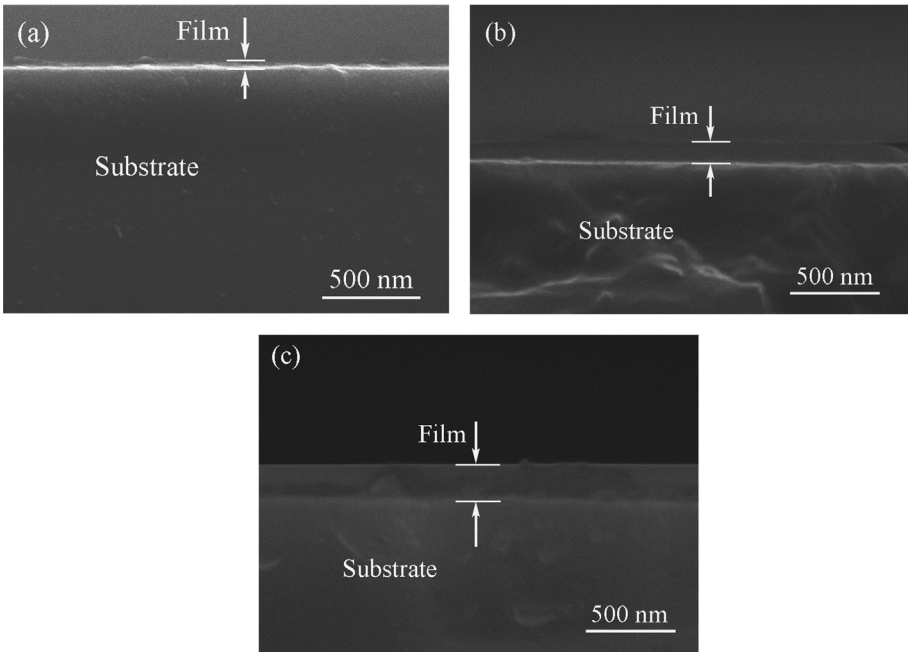

Fig. 1. Cross-section images of glass samples coated with (a) one-, (b) three- and (c) five-layer TiO_2 films.

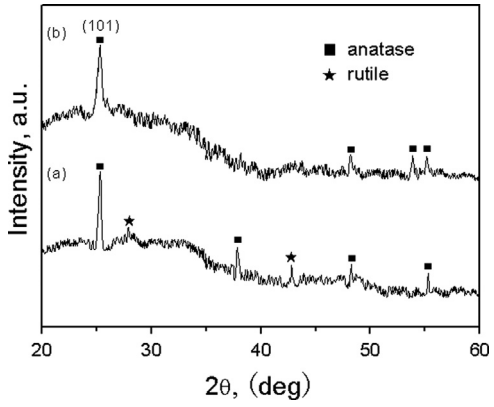

Fig. 2. XRD patterns of (a) undoped and (b) Ce^{3+}-doped TiO_2 film.

3.2. XRD analysis

Fig. 2 shows the XRD patterns of the TiO_2 films sintered at 500 °C for 2 h. It can be noticed that the undoped film mainly consists of anatase and a small amount of rutile crystals, while the Ce^{3+}-doped one was only composed of anatase crystals, indicating that Ce^{3+} doping inhibited the crystallization of the rutile phase. It can also be seen in Fig. 2 that partial amorphous phases existed in both kinds of the films, which was attributed to the fact that the content of titania was small and affected by the underlying glass substrates.

3.3. AFM analysis

The AFM morphology of the samples was displayed in Fig. 3. The average surface roughness was measured for the samples corresponding to the AFM images. It can be seen that the surface of the glass substrate had a number of micro-cracks and micro-holes, as well as remarkably high surface roughness (3.26 nm). By comparison, the surface of one-layer pure TiO_2 films was crack-free with the grain size less than 50 nm, as shown in Fig. 3 (b), indicating that liquid TiO_2 sol was immersed in and filled the micro-cracks and micro-holes on the glass surface during the dip coating. In the subsequent sintering process, the film smoothly and uniformly covered the glass substrate surface. The film surface consisted of small and compact TiO_2 nanoparticles with a conical shape. The particles were well distributed but the surface roughness was relatively high, showing an average surface roughness of 2.19 nm. Fig. 3(c) shows the morphology of the one-layer Ce^{3+}-doped TiO_2 nanofilm. Compared with Fig. 3(b), the film was even better distributed and more compact. Ce^{3+} doping obviously decreased the TiO_2 granularity, and the average surface roughness was 1.15 nm. Fig. 3(d) shows the morphology of the three-layer pure TiO_2 nanofilm. The grain size enlarged, and some bright, large, unevenly distributed particles were observed because of the clustering and accumulation of some TiO_2 crystallites during the preparation of the multi-layer film. Meanwhile, as shown in Fig. 3 (f), more clustering occurred on the surface of the five-layer pure TiO_2 nanofilm. Fig. 3(e) shows the morphology of the three-layer Ce^{3+}-doped TiO_2 nanofilm. The particles distribution was uniform and compact. Conical nanoparticles were uniformly connected. Compared with Fig. 3(e), the surface of the five-layer Ce^{3+}-doped TiO_2 nanofilm was very smooth, as shown in Fig. 3(g). The granularity of TiO_2 was enlarged and the distribution of TiO_2 nanoparticles was more uniform and compact. The average surface roughness was 0.28 nm.

The main reason why the Ce^{3+}-doped TiO_2 films shown more uniform morphology than that of pure TiO_2 films was due to that many oxygen vacancies existed in TiO_2 films during the sintering process, one part of Ce could either diffuse into interstitial vacancies or substitute for Ti at lattice points. This would inevitably lead to the expansion of TiO_2 lattices so that the lattice distortion energy quickly accumulated and

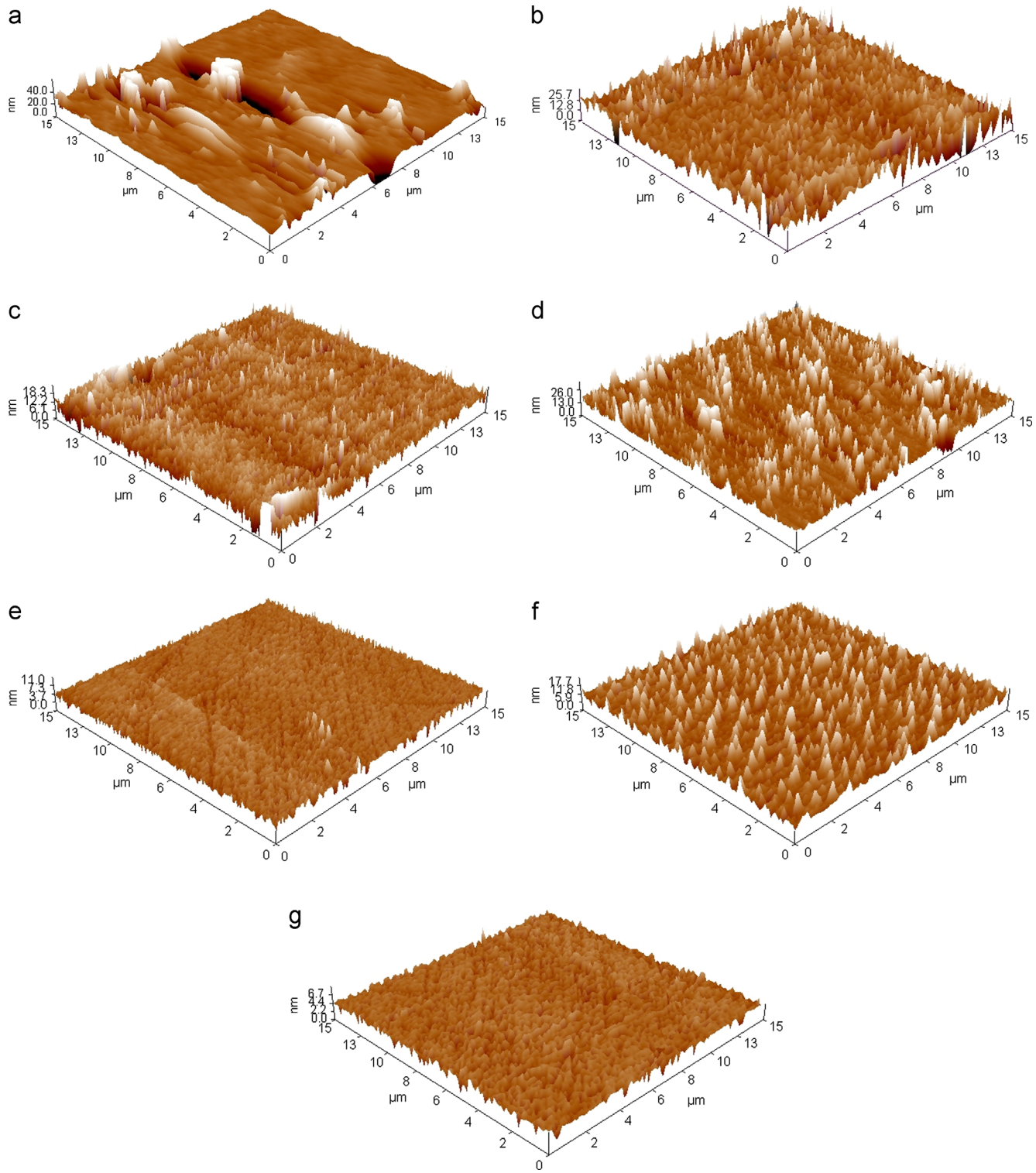

Fig. 3. AFM images of sample surfaces: (a) glass substrate, (b) one-layer undoped TiO_2 film, (c) one-layer Ce^{3+}-doped TiO_2 film, (d) three-layer undoped TiO_2 film, (e) three-layer Ce^{3+}-doped TiO_2 film, (f) five-layer undoped TiO_2 film and (g) five-layer Ce^{3+}-doped TiO_2 film.

eventually the growth of TiO_2 crystallites was inhibited. Another part of Ce not diffused into the lattice also would be enriched around the TiO_2 crystallites to resist growth of the crystallites [22]. Therefore, Ce^{3+}-doping could decrease the granularity of TiO_2 and improve the surface structure of the TiO_2 films.

3.4. Hardness of samples

Fig. 4 displays the surface hardness of the samples obtained from nanoindentation tests. The indentation depth of glass substrates, one-layer, three-layer, and five-layer films were about 200 nm, 20 nm, 60 nm and 100 nm, respectively.

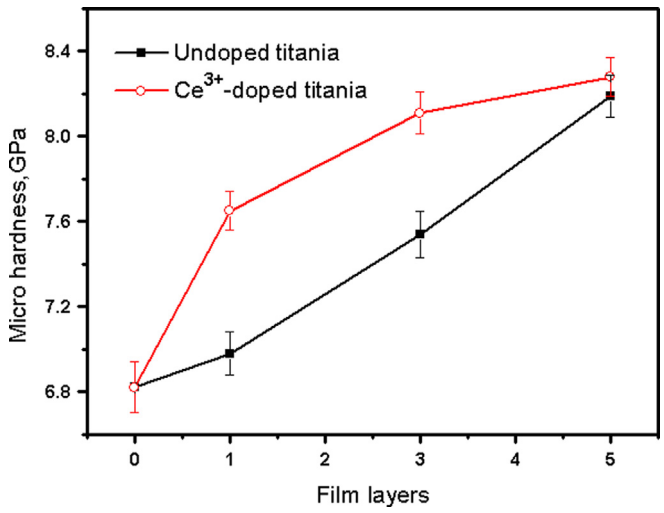

Fig. 4. Hardness of samples.

The surface hardness of uncoated glass substrate was about 6.8 GPa. While the surface hardness of the coated samples increased with the film layers and Ce^{3+} doping. After coating with five-layer pure TiO_2 nanofilm, the surface hardness of glass sample increased by more than 20% compared with that of the uncoated sample. This finding was due to higher hardness of TiO_2 films, and the surface structure of TiO_2 films improved with the increase of film thickness and Ce^{3+} doping, which could improve the surface hardness of the samples.

During the nanoindentation process, when a concentrated load was applied to the glass surface with a diamond indenter, the surface initially displayed elastic deformation followed by plastic deformation and cracks with increased load. With appropriate loads on the diamond indenter, indentation occurred on the glass surface and its size was taken as the basis for the hardness of the sample. The elastic and plastic deformation on the glass surface was associated with its low temperature viscosity. Furthermore, the low-temperature viscosity of glass was closely related to its surface composition and structure. Under higher shear loads, plastic deformation of glass occurred, and a certain relationship between the microhardness of glass and its viscosity existed. Namely, the hardness increased with increased viscosity [23]. Oxidizing materials such CaO, MgO, TiO_2, ZrO_2, ZnO and Al_2O_3 can increase the low-temperature viscosity of glass [24]. Therefore, the coating of TiO_2 film on the glass surface can improve the hardness of glass. In addition, with a compact glass surface structure, deformation did not easily occur under shear force and the hardness also improved. Fig. 3 shows that with increased film layers and Ce^{3+} doping, films surface became more uniform and compact. Therefore, the hardness improved with the increase of the film layers and Ce^{3+} doping.

Comparing the two hardness curves in Fig. 4 revealed that the surface hardness of the pure TiO_2 nanofilm rapidly increased with increased film layers. However, for the films doped with Ce^{3+}, the surface hardness gradually increased with the film layers. The reason was possibly due to the fact that the surface structure of pure TiO_2 nanofilms significantly changed with increased film layers. On the other hand, the surface structure of all Ce^{3+}-doped films were relatively uniform and compact, and the surface structure slightly changed with increased film layers, as shown in Fig. 3.

3.5. Tribological properties of samples

Fig. 5 shows the friction coefficient of the samples. The friction coefficient of glass substrate remarkably fluctuated, as shown in Fig. 5a. With the time prolonged, the fluctuation range decreased to a certain degree. The average friction coefficient of glass substrate was 0.37. It was due to that the brittle rupture and large abrasive particles were produced on the glass surface in the initial stage of sliding. These particles became grinding materials, amplifying the friction coefficient of the glass surface and exerting plowing effects. Then, the friction process soon entered the interior of the glass. Therefore, at the initial sliding, the friction coefficient remarkably fluctuated, and then, the particles were ground and the fluctuating range of the friction coefficient decreased.

Moreover, in the initial stage of sliding, the friction coefficients of the coated samples were extremely low. The friction coefficients of the samples coated with one-, three-, and five-layer pure TiO_2 nanofilms, as shown in Fig. 5b, d, and f, were 0.035, 0.030 and 0.027, respectively. Meanwhile, those for one-, three-, and five-layer TiO_2 nanofilms doped with Ce^{3+}, as shown in Fig. 5c, e, and g, were 0.031, 0.022, and 0.016, respectively. In addition, the fluctuation of the curves was insignificant. With the increase of film layers and Ce^{3+} doping, the friction coefficient became much more stable. In particular, for the five-layer Ce^{3+}-doped film, the friction coefficient was almost a horizontal line. This finding indicated that the TiO_2 nanofilms could remarkably reduce the friction coefficient of the glass surface, displaying an excellent wear resistance effect. Moreover, with increased film layers and Ce^{3+} doping, the effect became more obvious. With prolonged sliding time, the friction coefficient of the coated samples abruptly increased and then gradually fluctuated near 0.37. This result was due to the fact the high hardness and low friction coefficient of TiO_2 nanofilms resisted the abrasion of the steel ball in the initial stage. With the increase of time, the film ruptured and peeled off by the friction force. The stripping film fragments became the grinding materials that aggravated the failures of the film, thereby rapidly increasing the friction coefficient. Afterwards, the film was gradually worn through, the friction penetrated the glass substrate, and the friction coefficient gradually stabilized.

In addition, the wear life of TiO_2 nanofilms could be estimated by the duration from the beginning of the friction to the abrupt increase in the friction coefficient. As shown in Fig. 5b, d, and f, the wear lives of one-, three-, and five-layer pure TiO_2 nanofilms were 180, 220 and 240 s, respectively. Meanwhile, those of one-, three-, and five-layer TiO_2 nanofilms doped with Ce^{3+}, as shown in Fig. 5c, e, and g, were about 210, 260, and 300 s, respectively. Thus it could be seen, with increased film layers and Ce^{3+} doping, the friction coefficient of the samples gradually decreased and its wear-resistance property obviously increased.

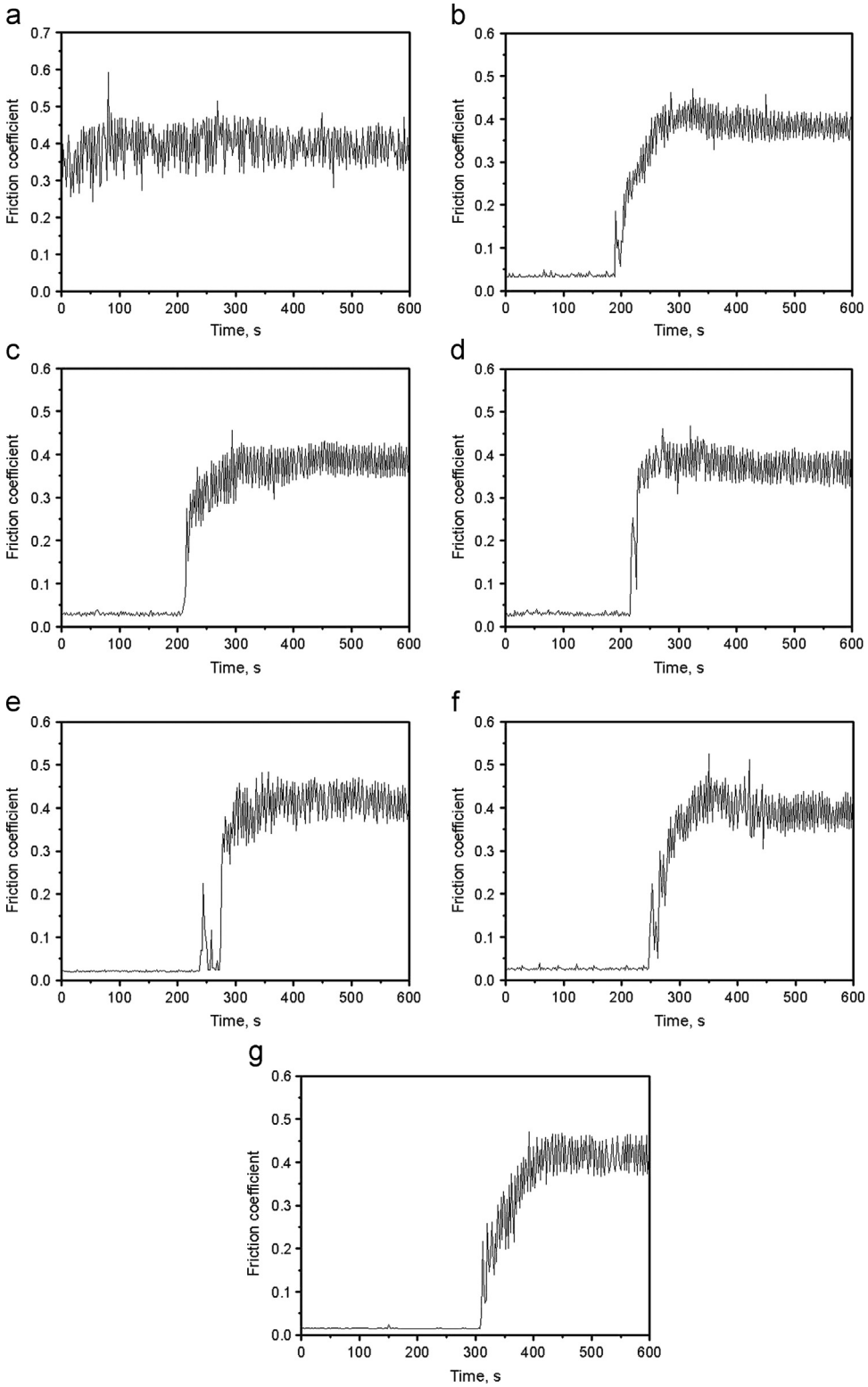

Fig. 5. Friction coefficient of samples: (a) glass substrate, (b) one-layer undoped TiO_2 film, (c) one-layer Ce^{3+}-doped TiO_2 film, (d) three-layer undoped TiO_2 film, (e) three-layer Ce^{3+}-doped TiO_2 film, (f) five-layer undoped TiO_2 film and (g) five-layer Ce^{3+}-doped TiO_2 film.

Fig. 6 demonstrates the worn surface of the samples. Based on the morphology of the uncoated glass substrate surface in Fig. 6(a), serious rupture occurred to the glass, generating a larger number of particles and pits such that a wide, deep, rough wear track was produced. For the wear tracks of the samples coated with TiO_2 nanofilms, fewer particles and narrow, shallow plows formed by slight scratching. The peeling film in a certain area produced a flaky plastic deformation belt, showing the features of fatigue wear.

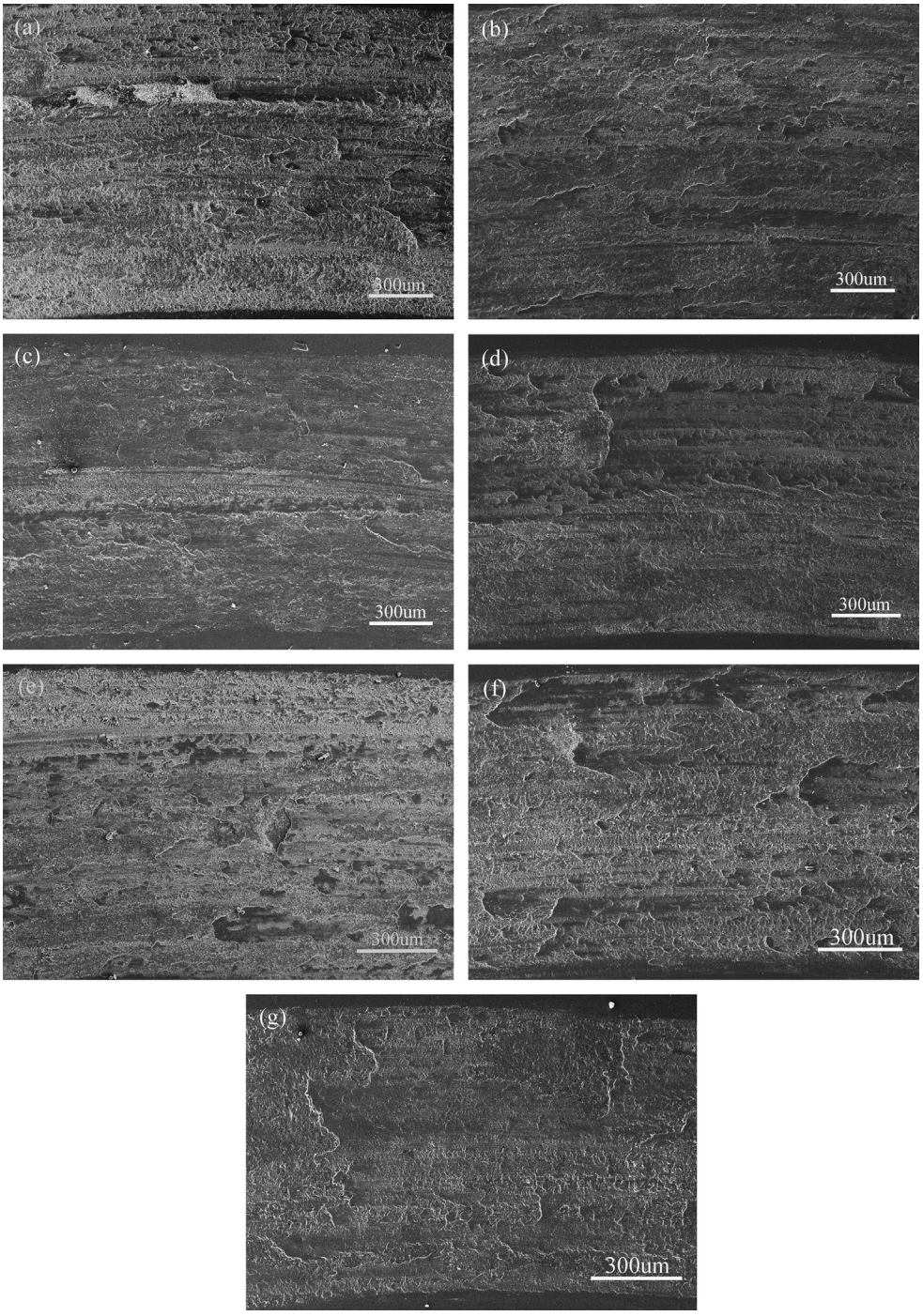

Fig. 6. Worn surface of samples: (a) glass substrate, (b) one-layer undoped TiO_2 film, (c) one-layer Ce^{3+}-doped TiO_2 film, (d) three-layer undoped TiO_2 film, (e) three-layer Ce^{3+}-doped TiO_2 film, (f) five-layer undoped TiO_2 film and (g) five-layer Ce^{3+}-doped TiO_2 film.

In addition, comparison of the widths of wear tracks revealed that with increased TiO_2 nanofilm layers and Ce^{3+} doping, the wear tracks of the sample surfaces gradually narrowed. This result also indicated that the role of TiO_2 nanofilms in the wear resistance of the glass surface evidently improved with increased TiO_2 nanofilm layers and Ce^{3+}-doping.

Similarly, after coating with TiO_2 nanofilms, the glass surface structure was remarkably improved. Meanwhile, with increased films thickness and Ce^{3+} doping, the film surfaces became more uniform and compact. The surface roughness significantly decreased, and the hardness of the sample improved. Thus, the friction coefficient obviously decreased with increased layers and Ce^{3+} doping. The wearing resistance was considerably improved.

4. Conclusions

Ce^{3+}-doped and undoped TiO_2 nanofilms with different layers were prepared on glass surface by a sol–gel method. With increased film thickness and Ce^{3+} doping in the film, the

surface structure of the samples remarkably improved and the surface roughness significantly decreased.

The surface hardness increased with increased layers and Ce^{3+} doping. After coating with five-layer pure and Ce^{3+}-doped TiO_2 nanofilms, the surface hardness of the samples improved by at least 20% and 22% compared with that of uncoated glass substrate. The friction-wear test demonstrated that the TiO_2 nanofilms coated on the glass substrate surface could be used as protective layers of the glass, presenting excellent wear resistance and friction-reducing effects. The friction coefficient of the uncoated glass surface was 0.37. But for the coated samples, the initial friction coefficient decreased to less than 10% of the uncoated glass. Meanwhile, the wear life of TiO_2 nanofilms greatly improved with the increase of the film thickness and the doping of Ce^{3+}. Furthermore, during the wearing process, the wearing mechanism of uncoated glass substrate included brittle rupturing and abrasive wearing, and the wearing forms of the coated glass surface mainly included peeling off and bruising.

Acknowledgments

This work is supported by Research Fund for the Doctoral Program of Higher Education of China (RFDP), 20111514120004, and by National Natural Science Foundation of China (NSFC), 51262021.

References

[1] U. Diebold, The surface science of titanium dioxide, Surface Science Reports 48 (2003) 53–229.
[2] R.S. Mane, O.S. Joo, W.J. Lee, et al., Unprecedented coloration of rutile titanium dioxide nanocrystalline thin films, Micron 38 (2007) 85–90.
[3] A. Yildiz, S.B. Lisesivdin, M. Kasap, et al., Electrical properties of TiO_2 thin films, Journal of Non-Crystalline Solids 354 (2008) 4944–4947.
[4] W.W. Xu, S.Y. Dai, L.H. Hu, et al., Influence of Yb-doped nanoporous TiO_2 films on photovoltaic performance of dye-sensitized solar cells, Chinese Physics Letters 23 (2006) 2288–2291.
[5] X.H. Wu, W. Qin, S. Wang, et al., Photoelectric properties of thin Eu^{3+}-doped TiO_2 filmssensitized by cis-$RuL_2(SCN)_2 \cdot 2H_2O$, Rare Metals 25 (2006) 169–172.
[6] D. Luca, D. Mardare, F. Iacomi, et al., Increasing surface hydrophilicity of titania thin films by doping, Applied Surface Science 252 (2006) 6122–6126.
[7] M. Afuyoni, G. Nashed, I.M. Nasser, TiO_2 doped with SnO_2 and studying its structural and electrical properties, Energy Procedia 6 (2011) 11–20.
[8] S. Gelover, P. Mondragón, A. Jiménez, Titanium dioxide sol–gel deposited over glass and its application as a photocatalyst for water decontamination, Journal of Photochemistry and Photobiology A: Chemistry 165 (2004) 241–246.
[9] N.P. Mellott, C. Durucan, C.G. Pantano, et al., Commercial and laboratory prepared titanium dioxide thin films for self-cleaning glasses: hotocatalytic performance and chemical durability, Thin Solid Films 502 (2006) 112–120.
[10] M. Dhayal, S.D. Sharma, Role of Ni doping in surface carbon removal and photo catalytic activity of nano-structured TiO_2 film, Surface Science 602 (2008) 1149–1154.
[11] M.L. Kääriäinen, D.C. Cameron, Titanium dioxide thin films, their structure and its effect on their photoactivity and photocatalytic properties, Thin Solid Films 517 (2009) 6666–6670.
[12] L.N. Protasova, E.V. Rebrov, T.S. Glazneva, et al., Control of the thickness of mesoporous titania films for application in multiphase catalytic microreactors, Journal of Catalysis 271 (2010) 161–169.
[13] Z.P. Yang, J.L. Yan, C.J. Zhang, et al., Enhanced removal of bilirubin on molecularly imprinted titania film, Colloids and Surfaces B: Biointerfaces 87 (2011) 187–191.
[14] Y.S. Ko, C.W. Koh, U.H. Lee, et al., Synthesis of mesoporous titania thin films with vertical pore channels and thick and crystalline walls, Microporous and Mesoporous Materials 145 (2011) 141–145.
[15] S.L. Feng, J.Y. Yang, M. Liu, et al., Hydrothermal growth of double-layer TiO_2 nanostructure film for quantum dot sensitized solar cells, Thin Solid Films 520 (2012) 2745–2749.
[16] W.M. Liu, Y.X. Chen, G.T. Kou, et al., Characterization and mechanical/tribological properties of nano Au–TiO_2 composite thin films prepared by a sol–gel process, Wear 254 (2003) 994–1000.
[17] I. Piwoński, Preparation method and some tribological properties of porous titanium dioxide layers, Thin Solid Films 515 (2007) 3499–3506.
[18] Q.Y. Jia, Y.J. Zhang, Z.S. Wu, et al., Tribological properties of anatase TiO_2 sol–gel films controlled by mutually soluble dopants, Tribology Letters 26 (2007) 19–24.
[19] E. Rayón, V. Bonache, M.D. Salvador, et al., Nanoindentation study of the mechanical and damage behaviour of suspension plasma sprayed TiO_2 coatings, Surface and Coatings Technology 206 (2012) 2655–2660.
[20] Y.X. Wang, H.L. Wang, F.Y. Yan, Effects of UV irradiation on tribological properties of nano-TiO_2 thin films, Surface and Interface Analysis 41 (2009) 399–404.
[21] Y. Wan, W.L. Chao, Y.F. Liu, et al., Tribological performance of fluoroalkylsilane modification of sol–gel TiO_2 coating, Journal of Sol-Gel Science and Technology 57 (2011) 193–197.
[22] Z.M. Shi, L. Yan, Phase transformation and crystal growth behaviors of La^{3+}/Ce^{3+}-doped TiO_2–20 wt% SnO_2 gels, Journal of Non-Crystalline Solids 354 (2008) 4654–4660.
[23] R.W. Douglass, Fifty Years of glass technology, Nature 212 (1966) 769–774.
[24] F.M. Ernsberger, Mechanical properties of glass, Journal of Non-Crystalline Solids 25 (1977) 293 (32).